NMR studies of G:A mismatches in oligodeoxyribonucleotide duplexes modelled after ribozymes

Masato Katahira, Hajime Sato, Ken Mishima, Seiichi Uesugi* and Satoshi Fujii[1]
Department of Bioengineering, Faculty of Engineering, Yokohama National University, Tokiwadai 156, Hodogaya-ku, Yokohama 240 and [1]Faculty of Pharmaceutical Science, Osaka University, Suita, Osaka 565, Japan

ABSTRACT

The structures of two oligodeoxyribonucleotide duplexes, the base sequences of which were modelled after both a hammerhead ribozyme and a small metalloribozyme, were studied by NMR. Both duplexes contain adjacent G:A mismatches; one has a PyGAPu:PyGAPu sequence and the other a PyGAPy:PuGAPu sequence. It is concluded on the basis of many characteristic NOEs that in both duplexes G:A base pairs are formed in the unique 'sheared' form, where an amino proton instead of an imino proton of G is involved in the hydrogen bonding, and G and A bases are arranged 'side by side' instead of 'head to head'. A photo-CIDNP experiment, which gives unique and independent information on the solvent accessibility of nucleotide bases, also supports G:A base pairing rather than a bulged-out structure of G and A residues. This is the first demonstration that not only the PyGAPu:PyGAPu sequence but also the PyGAPy:PuGAPu sequence can form the unique sheared G:A base pairs. Taking the previous studies on G:A mismatches into account, the idea is suggested that a PyGA:GAPu sequence is a minimum and essential element for the formation of the sheared G:A base pairs. The sheared G:A base pairs in the PyGAPu:PyGAPu sequence are suggested to be more stable than those in the PyGAPy:PuGAPu sequence. This is explained rationally by the idea proposed above.

INTRODUCTION

Since the discovery of ribozymes, studies to elucidate how ribozymes exert their enzymatic activities on the basis of their structures have been carried out [1–11]. It has been suggested that an A:G mismatch base pair is formed in some ribozymes and that the structure derived from this base pairing could play a crucial role in their enzymatic activities [12, 13]. For this reason, the G:A base pair has been studied in both oligodeoxyribonucleotide duplexes and oligoribonucleotide

duplexes. Particularly in oligodeoxyribonucleotide duplexes, several different types of G:A base pairs have been observed in both the crystal and solution states. 'head to head' G(anti):A(anti) [14, 15], G(anti):A(syn) [16], and G(syn):A(anti) [17, 18] have been observed. Recently, a 'sheared' G:A base pair was proposed [12, 19] , and results supporting this mode of base pairing are accumulating [20–22]. As the first step to elucidate the structure-activity correlation of ribozymes, we studied the structures of oligodeoxyribonucleotide duplexes containing G:A mismatches by NMR, the base sequences of which were modelled after ribozymes.

Figure 1 shows the base sequences of the oligodeoxyribo-nucleotide duplexes studied by NMR, duplexes 1 and 2, together with those of a hammerhead ribozyme [23] and a small metalloribozyme [24]. Duplex 1 is modelled after the bottom part of the hammerhead ribozyme, where the formation of G:A base pairs is suggested [13]. The first six bases of duplex 1 are identical to those of the bottom part of the hammerhead ribozyme. This part of duplex 1 is also nearly identical to the left part of the metalloribozyme, where the formation of G:A base pairs can be expected from the base sequence. As interesting G:A mismatches are incorporated in the first six bases, the bases 7 to 10 are chosen to form a self-complementary sequence in order to simplify NMR analysis. Thus, duplex 1 is suitable for probing the possibility of G:A base pair formation in ribozymes. An NMR study of a ribonucleotide duplex is much more difficult than one of a deoxy-ribonucleotide duplex due to the intense overlapping of resonances [25]. Therefore, we first studied corresponding oligodeoxyribo-nucleotide duplexes in order to obtain structural information on the G:A base pair.

It is notable that the base pairing geometry of G:A mismatches depends heavily on the neighbouring sequences. It was shown that the PyGAPu:PyGAPu sequence forms sheared G:A base pairs while the AGAT sequence forms a 'head to head' G(anti):A(anti) base pairs, and no duplex is formed (or GA bulges occur) for the GGAC sequence [21]. So far, nothing is known as to what kind of base pairing occurs for the PyGAPy:PuGAPu sequence, because only a series of self-complementary sequences

has been studied in detail by NMR. Therefore, it was of great interest, to investigate a non-self-complementary sequence, and duplex 2 was designed for this purpose. The first six bases of duplex 2 are the same as those of duplex 1, but duplex 2 is not self-complementary and thus has the PyGAPy:PuGAPu sequence.

Our studies demonstrate clearly that both duplexes 1 and 2 form unique 'sheared' G:A base pairs. A minimum and essential base sequence for the formation of the sheared G:A base pairs, PyGA:GAPu, has been proposed on the basis of our results. The stabilities of the sheared G:A base pairs in the PyGAPu:PyGAPu and PyGAPy:PuGAPu sequences are compared, and the difference in stability is explained rationally by application of the above rule.

MATERIALS AND METHODS

Each deoxyoligonucleotide strand, d(GGACGAGTCC), d(GGA-CGACATC) and d(GATGGAGTCC), was synthesized on a 10 μmol scale by the phosphoramidite coupling method with a model 392 DNA synthesizer (Applied Biosystems Co.). Each oligomer was purified and annealed as described previously [26].

For NMR measurement of non-exchangeable protons, a lyophilized sample was dissolved in 20 mM phosphate puffer (pH 7.0) containing 0.15 M NaCl. The solution was lyophilized and then dissolved in 0.4 ml of D_2O (99.96%). The concentration was 2.2 mM for each duplex. For measurement of exchangeable proton spectra, a $H_2O:D_2O$ mixture (9:1) was substituted for D_2O. DSS was used as an internal chemical shift reference.

NMR spectra were all recorded at 278−333 K with a Bruker AM-400 NMR spectrometer, except for a photo-CIDNP spectrum recorded with a JEOL GX-500 NMR spectrometer. Phase-sensitive NOESY [27] and HOHAHA [28] spectra were recorded by the time-proportional phase-increment method [29]. The mixing times for NOESY were 80, 100, 200, 300 and 500 ms, and the mixing time for HOHAHA was 40 ms. The repetition delay was 2.0 s. Two-dimensional spectra were recorded with 400−512 t_1 increments, being 96−160 free induction decays of 2 K data points per increment were collected. The t_1 and t_2 data were apodized with a $\pi/3$-shifted sine-bell function. The t_1 data were zero-filled to 1 K points. One-dimensional spectra in H_2O were accumulated with a 1−1 pulse sequence [30], and NOE difference spectra were obtained as described previously [26] with irradiation times of 100 and 300 ms. The photo-CIDNP difference spectrum was recorded as described previously [31] with laser irradiation of 0.8 W for 300 ms.

RESULTS

Figure 2 shows the one-dimensional ^1H NMR spectra and NOE difference spectra on irradiation of the imino protons of duplex 1 in H_2O at 288 K. The resonances of imino protons have been assigned sequentially on the basis of observed NOEs, as described previously [26]. It is notable that the imino proton of the G5 residue resonates at a high field, 10.29 ppm, well separated from the usual region, ~13 ppm, for a resonance of a hydrogen bonded imino proton of a G residue.

The resonances of non-exchangeable protons of duplex 1 have been assigned sequentially by analysis of two-dimensional NOESY and HOHAHA spectra in D_2O in the same way as reported for other oligodeoxyribonucleotide duplexes [32, 33], using previously established methods [34−40]. As an example, Figure 3 shows the expansion of the NOESY spectrum, indicating
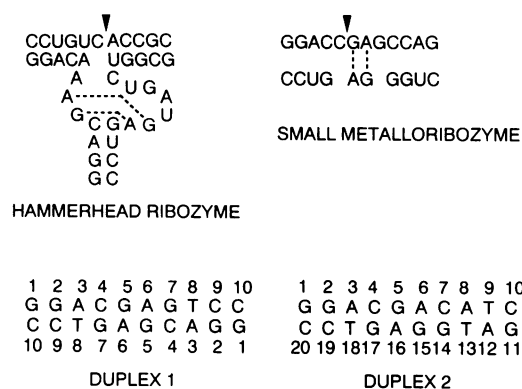

Figure 1. Base sequences of oligodeoxyribonucleotide duplexes studied by NMR, duplex 1 and duplex 2, together with the base sequences of a hammerhead ribozyme and a small metalloribozyme. Dotted lines indicate possible G:A base pairs. Arrows indicate positions of cleavage.
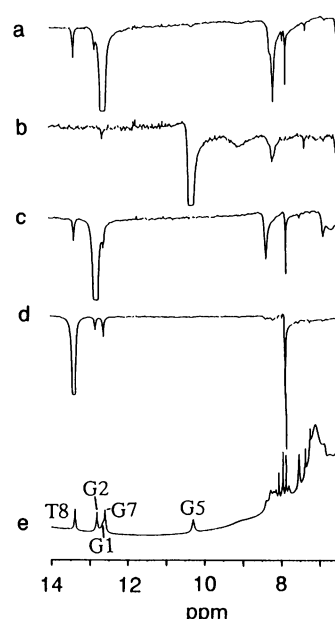

Figure 2. ^1H NMR spectrum with the assignments of the imino proton signals indicated by the residue numbers (e), and NOE difference spectra of duplex 1 at 288 K in the region of imino and aromatic proton resonances on 100 ms irradiation of the G7, G5, G2 and T8 resonances, respectively (a−d). The spectrum b is scaled up twice vertically for clarity.

the sequential assignments of H1' and H6/H8 through the H1' (i−1)−H6/H8 (i)−H1' (i) connectivities. It is notable that the connectivities are very weak at several points, C4H1'−G5H8, G7H8−G7H1' and A6H1'−G7H8, suggesting some structural perturbation around the G:A mismatches. In the same way, H2', H2', H3' and H4' were assigned, the assignments all being self-consistent and confirmed by HOHAHA spectra (data not shown). The assignments are summarized in Table 1.

The resonances of exchangeable and non-exchangeable protons of duplex 2 have been assigned in the same way. Figure 4 shows an imino proton spectrum with the assignments. The up-field shift of the imino proton resonances was also observed for the G5 and G15 residues in this case. Figure 5 shows the expansion of

Table 1. ^{1}H chemical shifts for duplex 1 at 298 K[a]

Residue	H6/H8	H2/H5/CH$_3$	H1'	H2'	H2''	H3'	H4'	imino/amino	
G1	8.04		5.62	2.45	2.58	4.77	4.13	12.66	
G2	7.87		5.59	2.67	2.79	4.98	4.34	12.83	
A3	8.12	7.91	6.19	2.49	2.78	4.97	4.41		
C4	6.93	4.90	5.87	1.38	1.98	4.76	4.15	6.60	8.25
G5	8.18		5.95	2.89	2.69	5.04	4.57	10.29	
A6	7.51	8.07	5.74	1.02	2.33	4.80	4.39		
G7	8.03		5.60	2.67	2.67	4.95	4.37	12.62	
T8	7.29	1.38	6.08	2.16	2.46	4.87	4.23	13.40	
C9	7.61	5.71	6.09	2.22	2.47	4.81	4.16	6.92	8.41
C10	7.71	5.78	6.20	2.27	2.27	4.53	4.02		

[a]At 288 K for imino and amino protons.

Table 2. ^{1}H chemical shifts for duplex 2 at 298 K[a]

Residue	H6/H8	H2/H5/CH$_3$	H1'	H2'	H2''	H3'	H4'	imino/amino	
G1	7.59		5.66	2.51	2.68	4.83	4.21	12.47	
G2	7.83		5.64	2.70	2.82	5.02	4.38	12.78	
A3	8.11	7.92	6.21	2.52	2.83	5.02	4.45		
C4	6.89	4.89	5.87	1.49	2.18	4.83	4.19	6.51	8.16
G5	8.19		5.99	2.92	2.60	5.11	4.52	10.19	
A6	7.66	7.78	5.47	1.66	2.46	b	4.33		
C7	7.55	5.78	6.06	2.19	2.37	4.97	4.10	6.98	8.13
A8	8.35	7.87	6.32	2.78	2.96	5.03	4.45		
T9	7.17	1.48	6.01	2.02	2.55	4.87	4.17	13.57	
C10	7.49	5.48	6.21	2.29	2.29	4.57	4.01		
G11	7.89		5.65	2.55	2.76	4.86	4.21	12.46	
A12	8.31	7.93	6.27	2.94	2.74	5.03	4.46		
T13	6.96	1.38	5.71	1.48	2.00	4.74	4.07	13.63	
G14	7.31		5.83	2.02	2.18	4.87	4.35	12.64	
G15	8.15		5.89	2.92	2.68	5.05	4.57	9.89	
A16	7.37	7.98	5.75	1.21	2.41	b	4.37		
G17	7.95		5.58	2.67	2.67	4.98	4.39	12.60	
T18	7.29	1.40	6.11	2.20	2.51	4.89	4.28	13.36	
C19	7.58	5.70	6.07	2.48	2.48	4.83	4.18	6.82	8.34
C20	7.56	5.59	6.18	2.29	2.29	4.57	4.01		

[a]At 288 K for imino and amino protons. [b]Not identified due to overlapping.

the NOEs spectrum with the sequential assignments of H1' and H6/H8 as an example. At several points weak connectivities are observed once again; A6H8−A6H1', A6H1'−C7H6, C7H1'−A8H8 and 16AH8−16AH1'. The assignments of duplex 2 are summarized in Table 2.

DISCUSSION

G:A mismatch structure of duplex 1

Three different types of base pairing have been observed for G:A mismatches in both the crystal and solution states; (a) 'head to head' G(anti):A(anti), (b) G(anti):A(syn), and (c) G(syn):A(anti). Recently, a new type of G:A base pair, (d) 'sheared' or 'side by side' G(anti):A(anti), was proposed and supported by experimental data. In terms of hydrogen bonding, the imino proton of G is a donor in (a) and (b), while the amino proton of G is a donor in (d), and no donor is assumed for G in (c). The imino proton of G5 of duplex 1 appears in the high field region at 10.29 ppm (Figure 2). A hydrogen-bonded imino proton signal of G usually appears at 12.5−13.5 ppm. This indicates that the imino proton of G5 is not involved in the hydrogen bonding. Thus, (a) and (b) are excluded as the G:A base pair of duplex 1. On irradiation of the imino proton of G5, a strong

NOE to A6H2 is expected in the case of (a) and to A6H8 in the case of (b), the intensity of which should be comparable to that between A3H2 and the imino proton of T8 in an A:T base pair. However, such a strong NOE was not observed, but weak NOEs were observed (Figure 2(b)), excluding the possibility of either (a) or (b) once again. It should be noted that NOEs to the amino protons of C4 (6. 60 and 8.25 ppm) were observed on irradiation of the imino proton of G5, although they were weak.

Before analyzing NOE results in detail, it was checked whether the factor ϱ^*/τ_c, can be assumed to be constant in the duplex [41]. Geometrically fixed distances, H2'−H2" and CH5−CH6, are used for this purpose. The intensities of H2'−H2" cross peaks in the NOESY spectrum with the mixing time of 100 ms are nearly identical for each residue, and the intensities of CH5−CH6 cross peaks are also nearly identical for each cytosine residue. Additionally, the intensities of H2'−H2' cross peaks relative to those of CH5−CH6 cross peaks are rationalized well by considering simple $1/r^6$-dependency of NOE cross peaks. These indicate that the factor ϱ^*/τ_c, can be assumed to be constant in the duplex.

In the syn conformation the H8(i)−H1'(i) distance is ~2.6 Å, which is comparable to the CH5(i)−CH6(i) distance (2.46 Å), while in the anti conformation this distance is ~3.8 Å, which
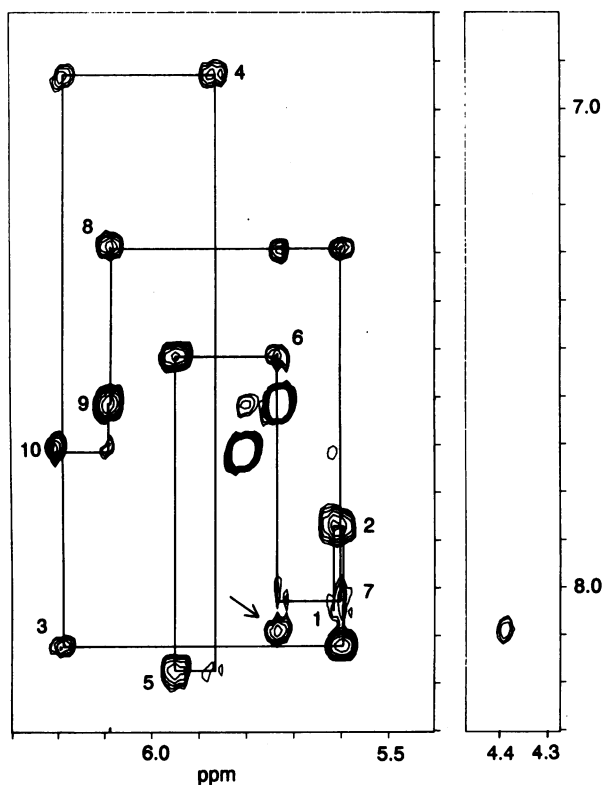
Figure 3. Expansion of the NOESY spectrum of duplex 1 obtained with a mixing time of 100 ms in a D_2O solution at 298 K. The lines show the H1′ (i−1)−H6/H8 (i)−H1′ (i) connectivities. The intraresidue cross peaks are labelled. An arrow indicates the interstrand A6H2−A6H1′ NOE. The interstrand A6H2−A6H4′ NOE is shown in the right panel.
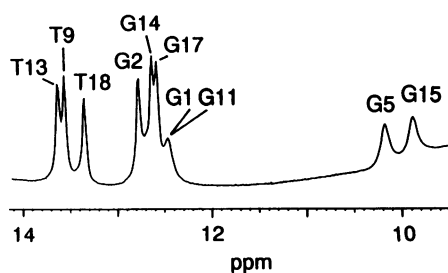

Figure 4. ¹H NMR spectrum of duplex 2 in the region of imino protons at 288 K with the assignments indicated by the residue numbers.

Figure 5. Expansion of the NOESY spectrum of duplex 2 obtained with a mixing time of 100 ms in a D_2O solution at 298 K with the H1′ (i−1)−H6/H8 (i)−H1′(i) connectivities. The intraresidue cross peaks are labelled. Arrows indicate the interstrand A6H2−A16H1′ and A16H2−A6H1′ NOEs.

is greater than the CH5(i)−CH6(i) distance [25]. The H8(i)−H1′(i) NOEs for G5 and A6 are much weaker than the CH5(i)−CH6(i) NOEs (Figure 3). In fact, the H8−H1′ distances calculated on the basis of the intensities of the cross peak in the NOESY spectrum with the mixing time of 100 ms by using geometrically fixed CH5−CH6 distance as the internal reference distance [32] are 3.6 Å for A6 and 3.4 Å for G5. When it is taken into account that the obtained distances tend to be underestimated ones due to spin diffusion [42], the results indicate clearly the anti conformation for both G5 and A6. Thus (b) and (c) are excluded as the G:A base pair of duplex 1. Thus (d) turns
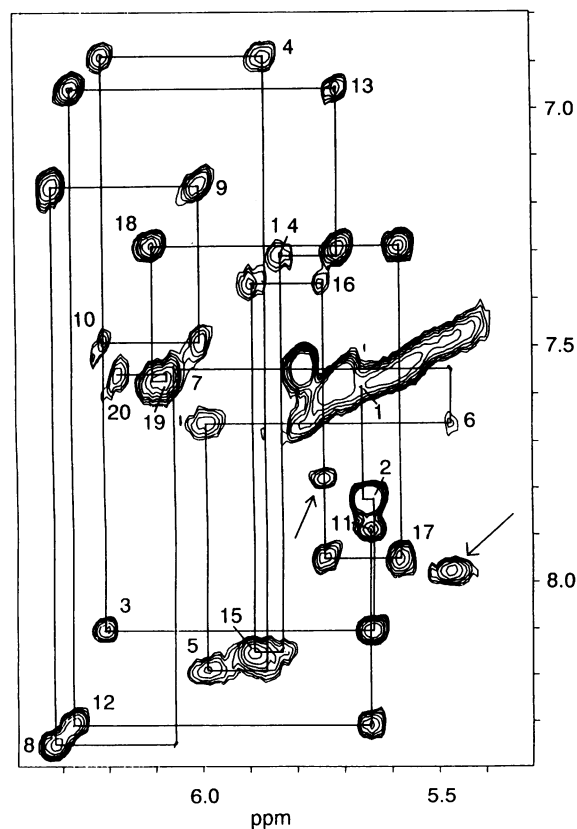
out to be the only base pair which is consistent with the experimental data.

As a consequence of unique base pairs of type (d), the mode of base stacking becomes extremely different from the standard one, as pointed out previously [12, 19−21] . This can be demonstrate easily by a simple model building study, as shown in Figure 6. Initially a model was constructed just by making two consecutive sheared G:A base pairs and minimizing the energy using X-PLOR [43] to avoid steric hindrance. It was seen that one G5 base is stacked on another G5 base of the other strand, and that one A6 base is stacked on another A6 base of the other strand, while the G5 base is not stacked on the A6 base of the same strand at all. This remarkable stacking mode was confirmed further by peculiar NOEs; A6H2−A6H1′ and A6H2−A6H4′ (Figure 3) . The intraresidue AH2−AH1′ and AH2−AH4′ distances are too long for any conformation to give solid NOEs [25]. Therefore, the observed NOEs should be interstrand NOEs. Such NOEs cannot be expected for the standard base stacking, while they are expected for the unique mode of base stacking shown in Figure 6, where the A6 residue of one strand is very close to another A6 residue of the opposite strand. Thus, the unique A6H2−A6H1′ and A6H2−A6H4′ NOEs strongly support a G:A base pair of the type (d). At this stage, the model was refined further by incorporating the information of the NOEs as the proximity of the corresponding protons. The unique stacking mode also gives a hint as to why the imino proton of G5 is visible, although it is not involved in the hydrogen bonding.
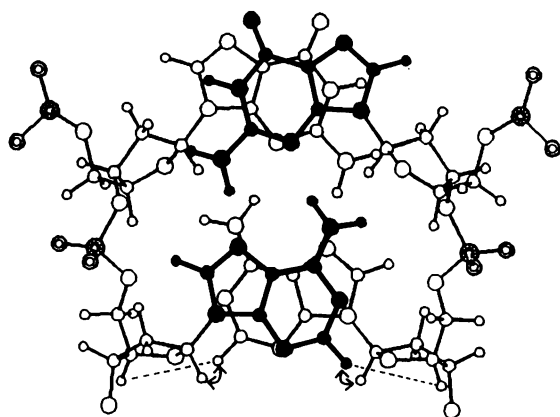
Figure 6. Mode of the base stacking model-built on the basis of the experimental observations for two consecutive G:A mismatch base pairs of duplex 1. The upper bases are shown as thick lines and closed circles. The proximity of interstrand A6H2−A6H1' and A6H2−A6H4' is indicated by double-headed arrows and dotted lines, respectively.

Figure 7. Photo-CIDNP difference spectra of duplex 1 at 293 K (bottom) and 333 K (top).

Probably, this is due to reduced accessibility of the imino proton to the solvent water.

Several resonances appear in unusually high field regions, A6H2' (1.02 ppm), C4H2' (1.38 ppm), and C4H5 (4.90 ppm), together with moderately upfield shifted C4H2" (I1.98 ppm), C4H6 (6.91 ppm), and A6H8 (7.49 ppm). These unusual chemical shifts were all observed for A6 or C4 residues which form the unique sheared G:A base pair or are located next to the sheared G:A base pair. It is suggested that the unusual mode of base stacking causes these upfield shifts through the ring current effect.

In addition to the unusually weak H6/H8−H1' connectivities found at several points (mentioned under Results), the following observations (data not shown) are supposed to also be in line with the unique positioning of the bases: H6/H8(i)−H2"(i−1) NOE is absent and H6/H8(i)−H2'(i−1) NOE is weak for the A6−G5 step, and H6/H8(i)−H2'(i−1) NOE is weak for the G5−C4 and G7−A6 steps, although they are generally strong to medium for other steps.

Photo-CIDNP is a unique NMR method for studying the solvent accessibility of proteins [44]. This method was successfully applied for the first time to the structural study of double stranded nucleic acids by us [31]. A base of a G residue gives a clear photo-CIDNP signal when it is exposed to solvent, while it does not when it is not exposed. Figure 7 shows the photo-CIDNP difference spectra of duplex 1 at 293 K (bottom) and 333 K (top). No CIDNP signal is observed at 293 K, while strong CIDNP signals are observed when the duplex is melted and the bases are exposed to the solvent by raising the temperature to 333 K. This indicates that all G bases including G5 are not solvent accessible at 293 K. The possibility of a bulged-out structure for the G:A mismatch, with the G5 and A6 bases flipped out of the duplex, which was observed for the GGAC sequence [21], was ruled out clearly by these independent NMR data. The photo-CIDNP results support the formation of a G:A base pair with the bases incorporated into the duplex.

Thus, it is concluded that unique sheared base pairs are formed for the G:A mismatches of duplex 1, which was modelled after a hammerhead ribozyme and a small metalloribozyme.
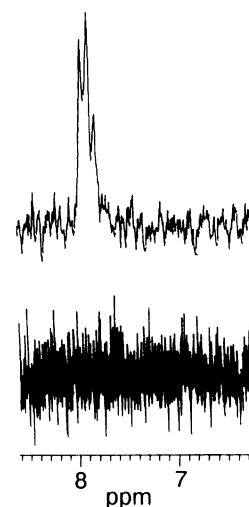
G:A mismatch structure of duplex 2

Duplex 2 was studied in the same way. The formation of two consecutive sheared G:A base pairs is concluded on the basis of the following series of observations, (1)−(6). (1) The imino protons of G5 and G15 resonate in the high field region, 10.19 ppm and 9.89 ppm, respectively. (2) Strong NOEs to neither H2 nor H8 of A6 and A16 residues are observed on irradiation of the imino protons of G15 and G5. (3) G5, A6, G15 and A16 all take on an anti conformation. (4) Characteristic NOEs of sheared base pairs are observed for interstrand A6H2−A16H1' A6H2−A16H4' , A16H2−A6H1' and A16H2−A6H4' . It is an advantage of the non-self-complementary nature of duplex 2 that these key interstrand NOEs can be unambiguously distinguished from intraresidue NOEs. (5) Extreme upfield shifts of resonances are observed for C4H2' (1.49 ppm), A6H2' (1.66 ppm), T13H2' (1.48 ppm), A16H2' (1.21 ppm), and C4H5 (4.89 ppm), together with a moderately upfield shifted C4H6 (6.89 ppm) signal. These are observed for the residues forming the unique base stacking or close to the unique base stacking. (6) In addition to the unusually weak H6/H8−H1' (connectivities found at several points (mentioned under Results), H6/H8(i)−H2'(i−1) NOE is absent and H6/H8(i)−H2"(i−1) NOE is very weak for the A6−G5 and A16−G15 steps, and a H6/H8(i)−H2'(i−1) NOE is very weak for the G5−C4, C7−A6, G15−G14 and G17−A16 steps, although they are generally medium to strong for other steps.

This study demonstrates for the first time that the PyGAPy:PuGAPu sequence can form sheared G:A base pairs. The PyGAPu:PyGAPu and PuGAPy:PuGAPy sequences have been examined as to their ability to form G:A base pairs in detail by NMR [12, 20, 21]. The PyGAPu:PyGAPu sequence forms sheared G:A base pairs, while the AGAT sequence forms 'head to head' base pairs, and the GGAC sequence forms no duplex (or GA bulges). However, it remains unanswered what happens for the PyGAPy:PuGAPu sequence, because only self-complementary sequences have been studied so far. This study answers this question, and has expanded the base sequence for which the possible formation of a sheared G:A base pair should be taken into account.

Essential base sequence for the formation of a sheared G:A base pair

It is interesting to note the outstanding difference that our CGAC:GGAG sequence forms sheared G:A base pairs, while the GGAC:GGAC sequence cannot form a duplex (or forms GA bulges) [21]. The GAC:GGA sequence is common in both the CGAC:GGAG and GGAC:GGAC sequences. Taking into account the facts that the PyGAPu:PyGAPu sequence and the PyGAPy:PuGAPu sequence form sheared G:A base pairs, as demonstrated for duplexes 1 and 2, but that the PuGAPy:PuGAPy sequence does not form sheared G:A base pairs, the idea is reached that the PyGAX:XGAPu sequence, or simply the PyGA:GAPu sequence is the minimum and essential element for the formation of sheared G:A base pairs. This kind of asymmetric sequence can be deduced only by studying a non-self-complementary sequence.

It is supposed that in addition to the excellent interstrand G−G and A−A stacking at the central GA sequence step, the stacking interaction at the PyG:APu sequence causes crucial stabilization for the formation of sheared G:A base pairs. An interaction at the PuG:APy step does not seem to cause sufficient stabilization for the formation of sheared G:A base pairs. The GGAC:GGAC sequence cannot form a sheared G:A base pair because it lacks the crucial PyG:APu interaction. The AGAT:AGAT sequence cannot form a sheared G:A base pair for the same reason. The AGAT:AGAT sequence can form 'head to head' G:A base pairs, possibly with the help of extra hydrogen bonding between the amino group of the G and the carbonyl-group of the T of the preceding A:T pair, as observed in the crystal state [15] and suggested previously [21]. The GGAC:GGAC sequence cannot make use of this extra hydrogen bonding, thus it forms no duplex.

Very recently the formation of the sheared G:A base pair is reported for d(TGTTTGGC):d(ACAAACA), with a terminal C residue left unpaired at the end [22]. This sequence is not an XGAX:XGAX type which gives two adjacent G:A base pairs. It is interesting that a single sheared G:A base pair is stable at the end of the duplex. Some different mechanism for the stabilization of the sheared G:A base pair may exist at the end of the duplex in this case.

Comparison of the stabilities of the sheared G:A base pairs in duplexes 1 and 2

It was also interesting to determine which sheared G:A base pairs are more stable between the PyGAPu:PyGAPu and PyGAPy:PyGAPu sequences. Although the sequence of duplex 2 is similar to that of duplex 1, in fact, the first to sixth base pairs are identical, the ninth C:G base pair in duplex 1 is replaced by a T:A base pair in duplex 2. Therefore, comparison of the stabilities of the sheared G:A base pairs is not straightforward, because the stability could be affected by this difference. However, it is still suggested that the sheared G:A base pair in the PyGAPu:PyGAPu sequence is more stable than that in the PyGAPy:PuGAPu sequence on the basis of the following observations. In the case of duplex 2, at 303 K the resonances of the imino protons of the G's in the central sheared G:A base pairs are very broad, almost disappearing, due to rapid exchange with water, while the resonances of imino protons of the other residues except for terminal residues remain solidly (data not shown). In the case of duplex 1, at this temperature, the resonance of the imino proton of the G in the central G:A base pair is clearly observed together with the resonances of the imino protons of the other residues except for terminal residues. This order of

stability is consistent with the results of previous thermodynamic analyses of a series of adjacent G:A mismatches [19] , although the mode of G:A base pair formation in the PyGAPy:PuGAPu sequence was not identified then.

It is very remarkable that the stability of the PyGAPu:PyGAPu sequence compared to that of the PyGAPy:PuGAPu sequence can be explained rationally on the basis of the proposed idea of an essential element for the formation of sheared G:A base pairs. The PyGAPu:PyGAPu duplex has two PyGA:GAPu segments, which partially overlap each other, preferable for the formation of sheared G:A base pairs. Thus, the two PyG:APu steps, probably through the stacking interaction, stabilize the consecutive sheared G:A base pairs. On the other hand, the PyGAPy:PuGAPu sequence has only one PyGA:GAPu sequence, and the PyG:APu step occurs only at one position. Therefore the sheared G:A base pair in the PyGAPu:PyGAPu duplex is more stable than that in the PyGAPy:PuGAPu duplex.

REFERENCES

1. Cech,T.R. (1987) *Science*, **236**, 1532−1539.
2. Uhlenbeck,O.C. (1987) *Nature*, **328**, 596−600.
3. Koizumi,M., Iwai,S. and Ohtsuka,E. (1988) *FEBS Lett.*, **228**, 228−230.
4. Ruffner,D.E., Stormo,G.D. and Uhlenbeck,O.C. (1990) *Biochemistry*, **29**, 10695−10702.
5. Perreault,J.P., Wu,T.F. , Cousineau,B., Ogilvie,K.K. and Cedergren,R. (1990) *Nature*, **344**, 565−567.
6. Heus,H.A., Uhlenbeck,O.C. and Pardi,A. (1990) *Nucleic Acids Res.* **18**, 1103−1108.
7. Pieken,W.A., Olsen,D.B., Benseler,F., Aurup,H. and Eckstein,F. (1991) *Nature*, **253**, 314−317.
8. Fu,D.J. and McLaughlin,L.W. (1992) *Proc. Natl . Acad. Sci USA*, **89**, 3985−3989.
9. Williams,D.M., Pieken,W.A. and Eckstein,F. (1992) *Proc. Natl. Acad. Sci. USA*, **89**, 918−921.
10. Taylor,N.R., Kaplan,B.E., Swiderski,P., Li,H. and Rossi,J.J. (1992) *Nucleic Acids Res.*, **20**, 4559−4565.
11. McCall,M.J., Hendry,P. and Jennings,A. (1992) *Proc. Natl. Acad. Sci. USA*, **89**, 5710−5714.
12. Li,Y., Zon,G. and Wilson,W.D. (1991) *Proc. Natl. Acad. Sci. USA*, **88**, 26−30.
13. Uesugi,S., Odai,O., Kodama,H., Hiroaki,H., Sakata,T. and Tanaka,T. (1992) In Sarma,R.H. and Sarma,M.H. (eds), *Structure & Function*, Adenine Press, New York, Vol II, pp. 143−158.
14. Kan,L.S., Chandrasegaran,S., Pulford,S.M. and Miller,P.S. (1983) *Proc. Natl. Acad. Sci. USA*, **80**, 4263−4265.
15. Prive,V.I., Heinemann,U., Chandrasegaran,S., Kan,L.S. Kopka,M.L. and Dickerson,R.E. (1987) *Science*, **238**, 498−504.
16. Brown,T., Hunter,W.N., Kneale,G. and Kennard,O. (1986) *Proc. Natl. Acad. Sci. USA*, **83**, 2402−2406.
17. Gao,X. and Patel,D.J. (1988) *J. Am. Chem. Soc.*, **110**, 5178−5182.
18. Brown,T., Leonard,G.A., Booth,E.D. and Chambers,J. (1989) *J. Mol. Biol.*, **207**, 455−457.
19. Li,Y., Zon,G. and Wilson ,W.D. (1991) *Biochemistry*, **30**, 7566−7572.
20. Chou,S.H. , Cheng,J.W. and Reid,B.R. (1992) *J. Mol. Biol.* **228**, 138−155.

21. Cheng, J.W., Chou,S.H. and Reid,B.R. (1992) *J. Mol. Biol.* **228**, 1037–1041.
22. Maltseva,T., Sandström,A. , Ivanova,I.M., Sergeyev,D.S., Zarytova,V.F. and Chattopadhyaya,L. (1993) *J. Biochem. Biophys. Methods*, **26**, 173–236.
23. Odai,O., Kodama,H., Hiroaki,H., Sakata,T., Tanaka,T. and Uesugi,S. (1990) *Nucleic Acids Res.*, **18**, 5955–5960.
24. Pan,T. and Uhlenbeck,O.C. (1992) *Nature*, **358**, 560–563.
25. Wüthrich,K. (1986) *NMR of Proteins and Nucleic Acids*. John Wiley and Sons, Inc.
26. Katahita,M., Sugeta,H., Kyogoku,Y., Fujii,S. Fujisawa,R. and Ken-ichi Tomita. (1988) *Nucleic Acids Res.* **17**, 8619–8632.
27. Jeener,L., Meier,B.H., Bachmann,P. and Ernst,R.R. (1979) *J. Chem. Phys.*, **71**, 4546–4553.
28. Davis,D.G. and Bax,A. (1985) *J. Am. Chem. Soc.*, **107**, 2821–2822.
29. Marion,D. and Wüthrich,K. (1983) *Biochem. Biophys. Res. Commun.*, **113**, 967–974.
30. Clore,G.M., Kimber,B.J. and Gronenborn,A.M. (1983) *J. Magn. Reson.*, **54**, 170–173.
31. Katahira,M., Sakaguchi-Katahira,R., Hayashi,F., Uesugi,S. and Kyogoku,Y. (1991) *J. Am. Chem. Soc.*, **113**, 8647–8651.
32. Katahira,M., Sugeta,H., Kyogoku,Y. and Fujii,S. (1990) *Biochemistry*, **29**, 7214–7222.
33. Katahira,M., Sugeta,H. and Kyogoku,Y. (1990) *Nucleic Acids Res.*, **18**, 613–618.
34. Reid,D.G., Salisbury,S.A., Bellard,S., Shakked,Z. and Williams,D.H. (1983) *Biochemistry*, **22**, 2019–2025.
35. Scheek,R.M., Russo,N., Boelens,R., Kaptein,R. and van Boom,J.H. (1983) *J. Am. Chem. Soc.*, **105**, 2914–2916.
36. Hare,D.R., Wemmer,D.E., Chou,S.H., Drobny,G. and Reid,B.R. (1983) *J. Mol. Biol.*, **171**, 319–336.
37. Feigon,J. Denny,W.A., Leupin,W. and Kearns,D.R. (1983) *Biochemistry*, **22**, 5930–5942.
38. Clore,G.M. and Gronenborn,A.M. (1983) *EMBO J.*, **2**, 2109–2115.
39. Clore,G.M. Lauble,H., Frenkiel,T.A. and Gronenborn,A.M. (1984) *Eur. J. Biochem.*, **145**, 629–636.
40. Weiss,M.A. Patel,D.J., Sauer,R.T. and Karplus,M. (1984) *Proc. Natl. Acad. Sci. USA*, **81**, 130–134.
41. Derome,A.E. (1987) *Modern NMR Techniques for Chemistry Research*. Pergamon Press.
42. Nilsson,L., Clore,G.M., Gronenborn,A.M., Brunger,A.T. and Karplus,M. (1986) *J. Mol. Biol.*, **188**, 455–475.
43. Brünger,A.T. (1990) *X-PLOR: A System for Cryslltallography and NMR*. Yale University Press, New Haven, CT.
44. Kaptein,R. (1982) *Biological Magnetic Resonance*. Plenum, New York, pp. 145–191.